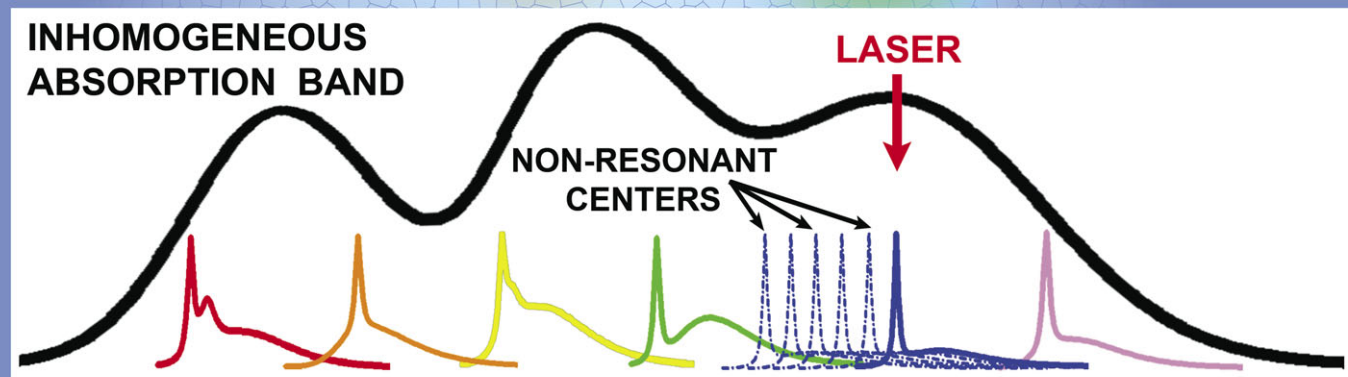
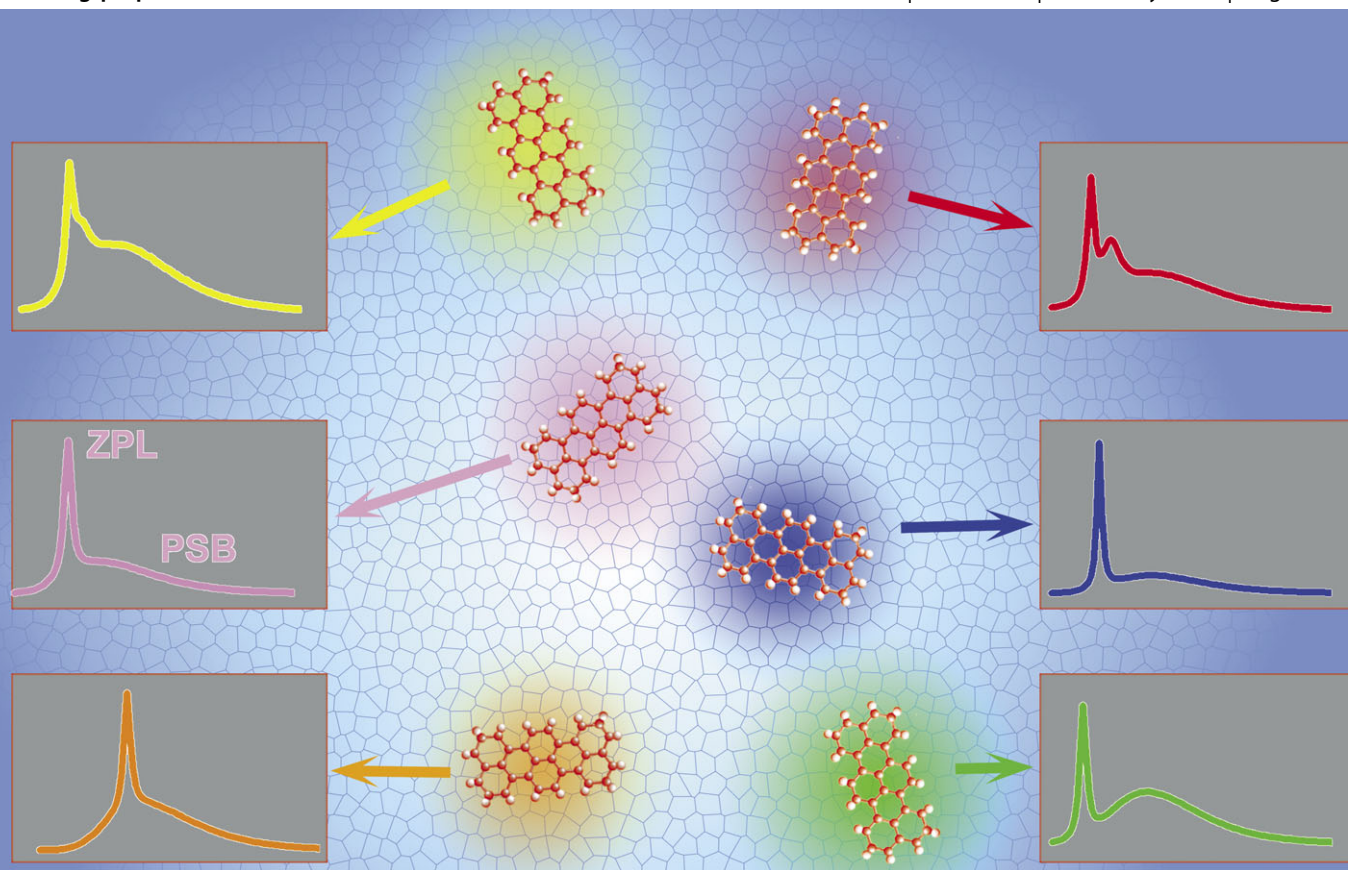


PCCP

Physical Chemistry Chemical Physics

www.rsc.org/pccp

Volume 13 | Number 5 | 7 February 2011 | Pages 1697–1900



Themed issue: Single-molecule optical studies of soft and complex matter

ISSN 1463-9076

COVER ARTICLE

Naumov *et al.*
Impurity spectroscopy at its ultimate limit: relation between bulk spectrum, inhomogeneous broadening, and local disorder

PERSPECTIVE

Tan and Yang
Seeing the forest for the trees: fluorescence studies of single enzymes in the context of ensemble experiments



1463-9076(2011)13:5;1-P

Cite this: *Phys. Chem. Chem. Phys.*, 2011, **13**, 1734–1742

www.rsc.org/pccp

PAPER

Impurity spectroscopy at its ultimate limit: relation between bulk spectrum, inhomogeneous broadening, and local disorder by spectroscopy of (nearly) all individual dopant molecules in solids

Andrei V. Naumov,^{*a} Aleksey A. Gorshelev,^a Yury G. Vainer,^a Lothar Kador^b and Jürgen Köhler^{*b}

Received 2nd September 2010, Accepted 22nd October 2010

DOI: 10.1039/c0cp01689f

We present a technique for the measurement of the low-temperature fluorescence excitation spectra and imaging of a substantial fraction of all single chromophore molecules (hundreds of thousands and even more) embedded in solid bulk samples as nanometre-sized probes. An important feature of our experimental studies is that the full information about the lateral coordinates and spectral parameters of all individual molecules is stored for detailed analysis. This method enables us to study a bulk sample in a broad spectral region with ultimate sensitivity, combining excellent statistical accuracy and the capability of detecting rare events. From the raw data we determined the distributions of several parameters of the chromophore spectra and their variations across the inhomogeneous absorption band, including the frequencies of the electronic zero-phonon lines, their spectral linewidths, and fluorescence count rates. Relationships between these distributions and the disorder of the matrix were established for the examples of two polycrystalline solids with very different properties, *n*-hexadecane and *o*-dichlorobenzene, and the amorphous polymer polyisobutylene. We also found spatially inhomogeneous distributions of some parameters.

1. Introduction

In 1993 *The Journal of Physical Chemistry* published a feature article by M. Orrit, J. Bernard, and R. I. Personov entitled “High-resolution spectroscopy of organic molecules in solids: From fluorescence line narrowing and hole burning to single-molecule spectroscopy”.¹ This paper reviewed the development of the optical spectroscopy of impurity centers in solids from the discovery of the narrow inhomogeneous lines in Shpol’skii matrices^{2–4} over the site-selective techniques of fluorescence line narrowing (FLN)^{5,6} and spectral hole burning (HB)^{6–8} up to single-molecule spectroscopy (SMS) which is completely free from ensemble averaging.^{9,10} The authors pointed out the great possibilities of all these methods for studying doped solids with different degrees of disorder. The site-selective methods FLN, HB, and SMS are particularly powerful, since they deal with the optical analogue of Mössbauer spectra—the zero-phonon lines (ZPLs) which

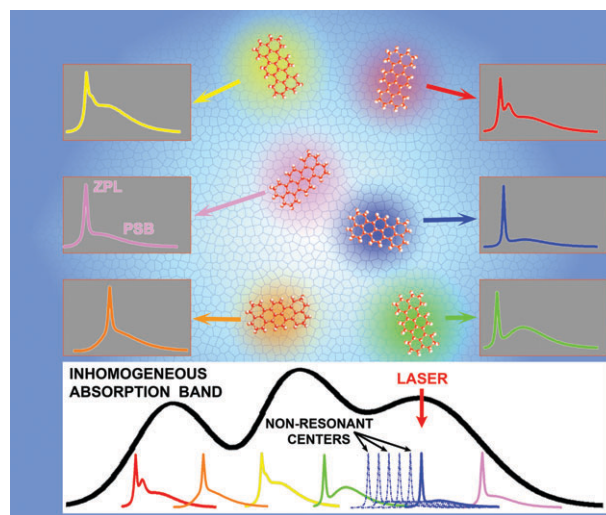


Fig. 1 Formation of the inhomogeneous absorption band of a doped solid at low temperatures as measured with fluorescence excitation spectroscopy. During the laser scan, the signal at each frequency position has contributions from chromophores excited resonantly through their zero-phonon lines and from chromophores which are excited non-resonantly through their phonon side bands (see also the classical illustration of the principles of laser selective spectroscopy in ref. 1).

^a *Molecular Spectroscopy Department, Institute for Spectroscopy, Russian Academy of Sciences, Troitsk, Moscow reg., 142190, Russia. E-mail: naumov@isan.troitsk.ru; Web: http://www.single-molecule.ru; Fax: +7 496 7510886; Tel: +7 496 7510236*

^b *Experimental Physics IV and Bayreuth Institute of Macromolecular Research (BIMF), University of Bayreuth, D-95440 Bayreuth, Germany. E-mail: juergen.koehler@uni-bayreuth.de; Web: http://www.ep4.phy.uni-bayreuth.de; Fax: +49 921-55-4002; Tel: +49 921-55-4000*

correspond to purely electronic transitions of impurity chromophores. Comprehensive studies have shown that in

doped solids at cryogenic temperatures individual optical spectra of impurities usually consist of narrow ZPLs and rather broad phonon sidebands (PSBs) which involve the creation or annihilation of matrix phonons (Fig. 1). The optical spectrum of a bulk sample (which is composed of the individual spectra of all the dopant molecules) is inhomogeneously broadened and, in most cases, unstructured, providing no detailed information about the dye–matrix system.

The parameters of a ZPL, in particular its spectral position and linewidth, are extremely sensitive to the local environment of the corresponding chromophore, which allows spectroscopists to use the chromophores as nanometre-sized spectral probes for studying internal processes in solids. FLN and HB, which record monochromatic sub-ensembles of ZPLs, proved to be powerful instruments for the investigation of crystals, glasses, polymers,^{1,6,11} laser materials,¹² quantum dots,¹³ nanostructures,¹⁴ proteins,^{15–18} light-harvesting complexes,¹⁹ and materials in bio-analytical and environmental chemistry.²⁰

In spite of their high spectral resolution, however, FLN and HB still provide data which are averaged over accidentally degenerate sub-ensembles of chromophores in a macroscopic volume ($\sim \mu\text{m}^3$ or larger), thereby hiding many important features of the individual spectra. This disadvantage is crucial when studying solids with complex structure^{21,22} because of their broad distributions of local parameters. A unique way to avoid the problem was presented by SMS which is not affected by ensemble averaging. SMS provides information about all the spectral parameters of individual ZPLs, including their frequency position within the inhomogeneous band²³ and allows one to directly observe slow spectral diffusion processes which show up as jumps or drifts on the frequency axis. During the last few years, SMS was demonstrated to provide information about truly local ($\sim \text{nm}$) properties of complex objects.^{24–31}

An important question in this context is the relationship between the distributions of local parameters of a solid matrix as obtained *via* SMS and the macroscopic spectral data of the same bulk sample as measured by conventional (ensemble) methods of laser selective spectroscopy (FLN and HB). This problem can be addressed by statistical analyses of individual spectral parameters of many SMs (see, *e.g.*, ref. 32–41). The combination of SMS and statistical data analysis yields the challenge to link the distributions of spectral positions, widths, and other characteristics of SM lines (which are determined by the local structure and dynamics) with macroscopic data. In order to exploit the full potential of this approach it is advisable to perform highly parallel measurements of large numbers of SM spectra using a SM luminescence microscope.^{42–47} Even more detailed information can be obtained by simultaneous measurements of the spectra and *spatial* coordinates of SMs.^{48–50} Until very recently, however, the number of SM spectra an experimentalist could measure and evaluate was far too small for performing adequate statistical analyses—from a few tens to a few thousands at the most.

In order to extend SM studies to macroscopically large numbers of SM spectral lines comparable with the total number of chromophores in the sample it is essential to take advantage of modern computing resources which allow one to store and process a large set of experimental data.⁵¹

Here we present the results of such an experiment in which the fluorescence excitation lines of hundreds of thousands and more SMs were recorded and the whole set of their individual spectral parameters and lateral coordinates were stored. For two polycrystalline matrices with very different characteristics (*n*-hexadecane and *o*-dichlorobenzene) and the amorphous polymer polyisobutylene (PIB) we demonstrate how the spectral parameters of the chromophores (frequencies, linewidths, count rates) vary across the inhomogeneous band and how they correlate with the spatial positions in the sample. Based on the huge data sets, we discuss the relationship between local matrix disorder and the distributions of SM data.

Thus, it appears feasible to continue the road outlined by Orrit *et al.*¹ to its culmination, *i.e.*, to measuring the “true” optical spectrum of a bulk sample by *recording the individual spectra of (nearly) all molecules* contributing to it.

2. Experimental

We have studied three organic solids with different levels of structural disorder: two polycrystalline materials with very different properties, *n*-hexadecane (*n*-Hex) and 1,2-(*o*-dichlorobenzene (*o*-DCB) doped with terylene (Tr), and the amorphous polymer polyisobutylene (PIB, $M_w = 420\,000 \text{ g mol}^{-1}$) doped with tetra-*tert*-butylterylene (TBT).

Samples of Tr/*n*-Hex and Tr/*o*-DCB were prepared by the following procedure: a drop of liquid solution of Tr in *n*-Hex or *o*-DCB (purchased from Sigma-Aldrich Co.) was placed between two thin microscope cover glasses at room temperature and quickly (during several seconds) cooled to liquid-nitrogen temperature (77 K) by inserting it into the pre-cooled cryostat. Amorphous PIB (purchased from Sigma-Aldrich Co.) was weakly doped with TBT synthesized in the Max-Planck-Institute for Polymer Research (Mainz, Germany)⁵² and kindly provided by Prof Th. Basché (University of Mainz, Germany). We used the same doped polymer material, which had been investigated before in SMS^{41,53,54} and PE^{55,56} experiments. The polymer sample was prepared by spin-coating a highly diluted solution of TBT/PIB in toluene onto a microscope slide. By adding pure PIB to the solution, the dye concentration was adjusted to a sufficiently low level, so the fluorescence images of SMs on the

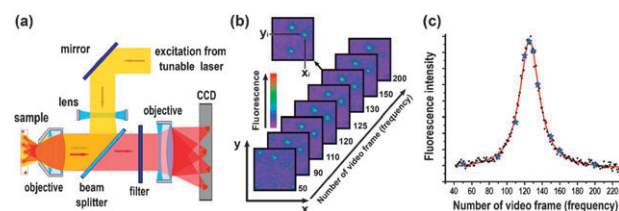


Fig. 2 (a) Scheme of the experimental setup and (b, c) illustration of the procedure of extracting single-molecule spectra and their parameters from a sequence of video frames. The luminescence images of the same set of single molecules in successive frames of a scan segment of 10 GHz width are identified according to their spatial coordinates x_i and y_i . (c) Fluorescence excitation spectrum of the i th molecule with coordinates x_i , y_i (dots and stars) and its fit with a Lorentz profile (solid line). Stars correspond to the video frames presented in part (b).

CCD chip could be clearly distinguished. The thickness of both polycrystalline and polymer films was between 0.5 and 1 μm and the corresponding total number of SMs within a scan segment (see below) was between a few tens and a few hundreds.

The experimental setup was a home-built epi-illuminated luminescence microscope with multi-channel data acquisition using a CCD camera (Fig. 2a). It allowed us to record simultaneously the fluorescence of all SMs which were in the field of view of the microscope objective and whose electronic 0–0 transition frequencies were in resonance with the exciting laser light. Automated data processing was performed with the specially developed software⁵⁷ used earlier in ref. 51 and ref. 58–60.

The setup has already been described in detail (see, *e.g.*, ref. 61). A tunable single-frequency ring dye laser (Coherent CR699-21 with auto-scan controller) operating with Rhodamine 6G in the spectral region between 565 and 591 nm (spectral bandwidth including jitter less than 2 MHz) was the excitation light source. The sample was placed in the focal plane of a microscope objective (Microthek, NA 0.9) which collected and collimated the luminescence of the chromophores. Sample and objective were immersed in superfluid helium in a He-4 bath cryostat cooled to 1.5 K. The sample was illuminated from the front side with the laser beam weakly focused to a spot of $\sim 80 \mu\text{m}$ diameter corresponding to the field of view of the objective. The fluorescence from the sample was imaged onto a thermoelectrically cooled highly sensitive EM-CCD camera (iXON, Andor Technology). Residual excitation light was suppressed with the combination of a band-pass interference filter (HQ610PL or similar) and a Schott RG610 glass filter.

Scanning of the laser frequency over the whole wavelength range accessible with Rhodamine 6G was accomplished with the auto-scan control box. It performed successive scans over 10 GHz intervals, in the following referred to as scan segments $\Delta\tilde{\nu}$, which were stacked. Each $\Delta\tilde{\nu}$ comprised 1000 frequency points with exposure time 10 ms per point (video frame). For recording the fluorescence images of SMs we read out only part of the CCD chip with size 100×100 pixels for Tr/*n*-Hex and the same area, yet, with 2×2 binning for Tr/*o*-DCB and TBT/PIB, corresponding to sample areas $\sim 70 \times 70 \mu\text{m}$.

In each scan segment, the individual fluorescence images and ZPLs were recorded synchronously for all SMs located in the imaged sample area (Fig. 2b). All the detected SM spectra were stored together with the following parameters obtained by fitting with a Lorentz function

$$I(\omega) = I_{\min} + \frac{2A_{\text{fluo}}}{\pi} \frac{\gamma}{4(\omega - \omega_0)^2 + \gamma^2}, \quad (1)$$

“offset” I_{\min} (noise background), “center” ω_0 (frequency position of the signal maximum within the segment), “linewidth” γ (full width at half-maximum), “area” A_{fluo} (integral fluorescence signal of the SM excluding noise floor), and $I_{\max} = 2A_{\text{fluo}}/\pi\gamma$ (fluorescence count rate at signal maximum). It is important that this data pool contained, in addition, the lateral coordinates $\{x_i, y_i\}$ of the detected chromophores. They were determined by locating the *center*

of gravity of the corresponding fluorescence images on the CCD chip.⁵¹ The experimental data showed that Lorentzian profiles are a good approximation for most SM spectral lines in solids, especially in polycrystalline samples. In the presence of strong spectral-diffusion processes and/or fluorescence blinking, this approximation is not as good but can still be used for data evaluation (see Section 6 for more details).

For further data processing the following parameters were calculated for each segment with spectral width $\Delta\tilde{\nu}$ (we used $\Delta\tilde{\nu} = 10$ GHz, but other values may be chosen as well):

- $\tilde{\nu}$ —wave number corresponding to the beginning of the segment (or corresponding laser wavelength λ);
- N_{SM} —number of SMs recorded within the segment;
- $\bar{\gamma}$ —average linewidth of the SM spectra in the segment;

$$\bar{\gamma} = \frac{1}{N_{\text{SM}}} \sum_{i=1}^{N_{\text{SM}}} \gamma_i \quad (2)$$

- \bar{I}_{\max} —average maximum fluorescence count rate

$$\bar{I}_{\max} = \frac{1}{N_{\text{SM}}} \sum_{i=1}^{N_{\text{SM}}} (I_{\max})_i \quad (3)$$

- A_{sum} —integral fluorescence signal from all SMs in the segment (sum of the integrated signals of all SMs whose fluorescence images were recognized)

$$A_{\text{sum}} = \sum_{i=1}^{N_{\text{SM}}} (A_{\text{fluo}})_i \quad (4)$$

These parameters, as functions of the spectral position $\tilde{\nu}$, $N_{\text{SM}}(\tilde{\nu})$, $\bar{\gamma}(\tilde{\nu})$, $\bar{I}_{\max}(\tilde{\nu})$, and $A_{\text{sum}}(\tilde{\nu})$, were obtained for all three samples Tr/*n*-Hex, Tr/*o*-DCB, and TBT/PIB. Besides, various statistical analyses of *individual* spectral parameters of the SMs were performed as detailed below.

With the developed technique it was also easily possible to measure the conventional high-resolution fluorescence excitation spectrum $F(\tilde{\nu})$. To this end the fluorescence signals in the working area (100×100 pixels) of the CCD chip were simply summed up over all frames in each segment, without SM recognition and without noise reduction. Here the width $\Delta\tilde{\nu}$ of the scan segments determines the spectral resolution. Of course, it is readily possible to achieve a much better resolution (down to the laser linewidth of about 2 MHz) by performing the sum over smaller spectral ranges rather than the whole segment.

3. Evaluation of the experimental data

The shape of the inhomogeneous absorption band of dopant chromophores in a solid is directly related to the structural properties of the solid.^{62–64} A characterization of this relationship is almost impossible with conventional methods of laser selective spectroscopy—FLN and HB, because these techniques average over large sub-sets of chromophores in a macroscopic volume. Here we demonstrate an experimental procedure for a detailed study of the inhomogeneous band by measuring the fluorescence excitation spectra of a large ensemble (hundreds of thousands) of *individual* chromophore molecules in the field of view of the microscope. It is based on a detailed analysis of the above-defined functions $N_{\text{SM}}(\tilde{\nu})$,

$A_{\text{sum}}(\tilde{\nu})$, $F(\tilde{\nu})$, $\bar{\gamma}(\tilde{\nu})$, and $\bar{I}_{\text{max}}(\tilde{\nu})$, which have the following physical meaning.

$N_{\text{SM}}(\tilde{\nu})$ denotes the number of individual molecules detected in a scan segment with spectral position $\tilde{\nu}$. Thus, it represents the distribution of the ZPL frequencies within the inhomogeneous absorption band. $N_{\text{SM}}(\tilde{\nu})$ is related, but not equal, to the high-resolution fluorescence excitation spectrum of a bulk sample as measured by conventional laser spectroscopy. The differences are due to the fact that the widths, areas, and even shapes of individual SM spectra can be very different, and the distributions of their parameters across the inhomogeneous band may be quite non-uniform.⁶⁵ Hereafter we will call $N_{\text{SM}}(\tilde{\nu})$ the *spectral density* of SMs.

Also $A_{\text{sum}}(\tilde{\nu})$ is related to the macroscopic high-resolution fluorescence excitation spectrum. It is the frequency dependence of the sum of all integrated SM spectra within a scan segment $\Delta\tilde{\nu}$. The process of recognition of SM fluorescence images implies the selection of signals which are higher than the background noise level and show a pronounced spectral dependence as expected for narrow fluorescence excitation lines (Fig. 2c). Thus, $A_{\text{sum}}(\tilde{\nu})$ is not completely equivalent to the fluorescence excitation spectrum of a bulk sample either: the important difference is that $A_{\text{sum}}(\tilde{\nu})$ does not contain the PSBs of the chromophores. Hence, it can be referred to as the *phononless absorption band*.

The function $F(\tilde{\nu})$ is the fluorescence excitation spectrum comprising the whole Stokes-shifted fluorescence of all impurities in a selected area, including the signals of non-resonant centers which are excited *via* their (broad) PSBs and whose emission is very low (see Fig. 1). As was already demonstrated in ref. 65, $F(\tilde{\nu})$ can be measured on samples with extremely low dye concentration in which SM signals are resolved. In ref. 65 the information about individual SM spectra was not considered, however.

The dependences $\bar{\gamma}(\tilde{\nu})$ and $\bar{I}_{\text{max}}(\tilde{\nu})$ represent the averaged values of the SM spectral linewidths and maximum fluorescence count rates, respectively, as a function of the spectral position within the inhomogeneous profile. Averaging is performed over a scan segment $\Delta\tilde{\nu}$.

We wish to stress again that the giant set of experimental data which comprises the spatial coordinates and complete spectra of all detected SMs allows us to perform a large variety of statistical analyses including, *e.g.*, the calculation of averages and correlations. In the following we will demonstrate some of the possibilities of this method.

4. Polycrystalline *n*-hexadecane doped with terrylene

Linear alkanes doped with dye molecules form polycrystalline Shpol'skii systems which are characterized by very narrow inhomogeneous bands. The matrices *n*-tetradecane and *n*-hexadecane, which belong to this class, had been investigated with single-molecule spectroscopy before.^{32,66–70} We have revisited this study for *n*-hexadecane with our technique by recording a huge number (105 332) of SM spectra in the spectral region 17 200–17 500 cm^{-1} . The total duration of this experiment was about 4.5 hours. The “pure measuring time” (time of the laser scans) was obviously shorter, about 2 h

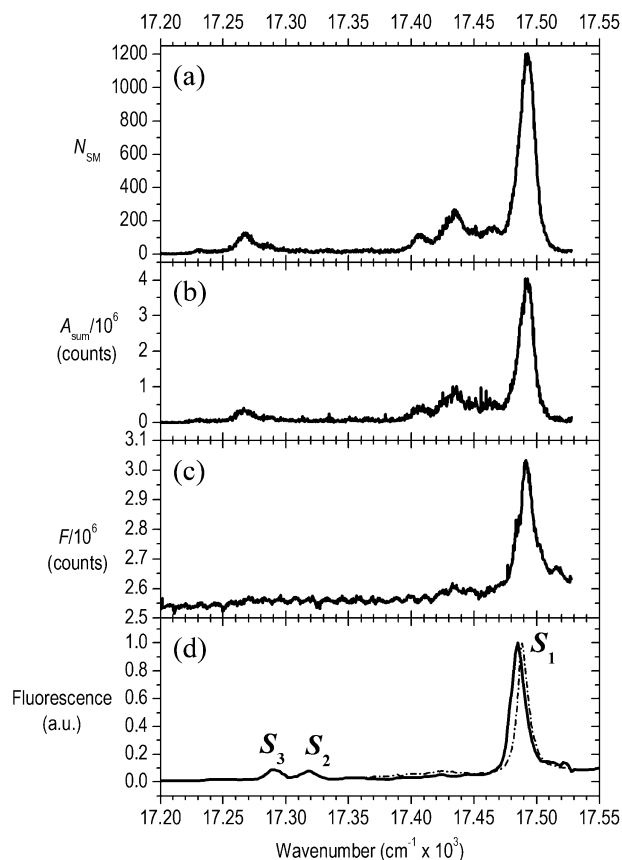


Fig. 3 (a) Spectral density $N_{\text{SM}}(\tilde{\nu})$ and (b) phononless absorption band $A_{\text{sum}}(\tilde{\nu})$ as measured for 105 332 terrylene molecules in polycrystalline *n*-hexadecane at $T = 1.5$ K. Scan segment $\Delta\tilde{\nu}$, 10 GHz. (c) High-resolution fluorescence excitation spectrum $F(\tilde{\nu})$ as measured in the same sample under identical conditions. (d) Bulk fluorescence excitation spectra of the same system as measured in ref. 71 (dash-dotted line) and ref. 72 (solid line) by conventional laser spectroscopy at $T = 4.2$ K. S_1 , S_2 , and S_3 represent the positions of resolved sites. The inhomogeneous width of the main site S_1 is ~ 12 cm^{-1} . For the definition of the functions $N_{\text{SM}}(\tilde{\nu})$, $A_{\text{sum}}(\tilde{\nu})$, and $F(\tilde{\nu})$ see main text.

50 min; it can easily be calculated from the data of the experimental procedure given in Section 2 (total scan range, 350 cm^{-1} ; scan segment, 10 GHz; number of frequency points per scan segment, 1000; exposure time per frequency point, 10 ms). Taking into account the typical SM spectral linewidths for Tr/*n*-Hex at $T = 1.5$ K (50–200 MHz), one can calculate the time for recording a SM spectral line as 50–200 ms.

Fig. 3a–c shows the experimental data $N_{\text{SM}}(\tilde{\nu})$, $A_{\text{sum}}(\tilde{\nu})$, and $F(\tilde{\nu})$, respectively. For comparison we present in Fig. 3d two bulk fluorescence excitation spectra of the same system as measured by conventional laser spectroscopy.^{71,72}

The positions of the main site S_1 ($\sim 17 492$ cm^{-1}) agree well in all spectra. Two sites of lower intensity, S_2 (17 320 cm^{-1}) and S_3 (17 290 cm^{-1}), which are clearly resolved in Fig. 3d are not visible in our data. Instead, $N_{\text{SM}}(\tilde{\nu})$ and $A_{\text{sum}}(\tilde{\nu})$ show at least 3 peaks in the region 17 220–17 300 cm^{-1} . The fine structure of $N_{\text{SM}}(\tilde{\nu})$ and $A_{\text{sum}}(\tilde{\nu})$ on the red side of S_1 (17 400–17 467 cm^{-1}) is much more pronounced than in $F(\tilde{\nu})$ and in the bulk spectra. In particular in $N_{\text{SM}}(\tilde{\nu})$ one can identify at least 3 peaks which are almost hidden in the latter.

The differences of the bulk fluorescence excitation spectra in Fig. 3d between each other and with respect to our spectrum $F(\tilde{\nu})$ (Fig. 3c) can be ascribed to different experimental parameters (*e.g.*, temperature or spectral resolution) and/or slightly different conditions of sample preparation and freezing.

An important feature of $N_{\text{SM}}(\tilde{\nu})$ and $A_{\text{sum}}(\tilde{\nu})$ is the complete absence of phonon sidebands, which are pronounced on the blue side of $F(\tilde{\nu})$ and the bulk spectra, especially close to the main site S_1 . These signals are due to molecules which are excited non-resonantly (*i.e.*, through their PSBs); hence, they are blue-shifted with respect to the main (ZPL) bands. In the high-resolution spectra of the bulk samples^{71,72} their contribution is significant (Fig. 3d), and also in our spectrum $F(\tilde{\nu})$ the PSB on the high-energy side of S_1 is well visible (Fig. 3c). In the “synthetic” distributions $N_{\text{SM}}(\tilde{\nu})$ and $A_{\text{sum}}(\tilde{\nu})$ they do not show up for two reasons: the Debye–Waller factor of the optical transition is high at 1.5 K and the PSBs are much broader than the ZPLs. Hence, a SM excited *via* its PSB emits a fluorescence signal which is too weak and varies too slowly with laser frequency to be recognized in the data evaluation procedure (compare Fig. 2).

The most impressive advantage of our “*all-single-molecules*” detection technique is the possibility to look inside the microscopic nature of a spectral site and its relation to the sample structure. We consider especially site S_1 . The enlarged central part of its inhomogeneous spectrum is plotted in Fig. 4a. It had always been assumed in the previous studies that this spectral site corresponds to a unique incorporation of the Tr molecule in the *n*-Hex matrix. With our technique we can calculate the spatial (lateral) distribution of the SMs forming the site. It was a big surprise that they can be roughly divided into two groups. Fig. 4b and c show the spatial density of Tr molecules whose spectra are located in the low-frequency (Fig. 4b) and the high-frequency (Fig. 4c)

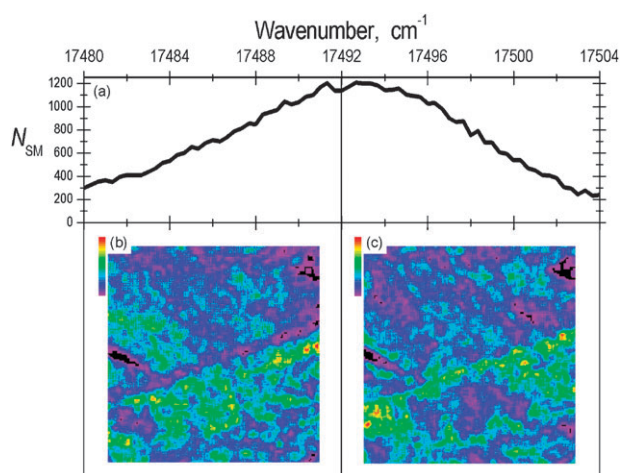


Fig. 4 (a) Spectral density $N_{\text{SM}}(\tilde{\nu})$ of Tr molecules in polycrystalline *n*-hexadecane at $T = 1.5$ K in the spectral region of site S_1 . (b, c) Color-coded topograms representing the spatial density of SMs with different spectral positions in the sample plane: Parts (b) and (c) correspond to ZPLs in the spectral interval 17480–17492 cm^{-1} and 17492–17504 cm^{-1} , respectively. The spatial density reaches values up to ~ 200 molecules per μm^3 (red color in the topograms).

wing of S_1 , respectively. Both distributions mark identical structures in the polycrystalline sample, but they show a pronounced anti-correlation with each other. We ascribe this result to the presence of a sub-site structure of peak S_1 , which had never been discussed so far. A possible interpretation is that the *n*-Hex crystal provides two slightly different accommodations for the Tr molecule. A clarification may be possible with the help of crystallographic calculations.

5. Polycrystalline *o*-dichlorobenzene doped with terrylene

Quickly frozen *o*-dichlorobenzene doped with terrylene was recently found as a new system for SMS.^{51,73} It is polycrystalline like Tr/*n*-Hex, yet, exhibits very different spectroscopic properties. Tr in *o*-DCB shows SM spectral dynamics typical for crystalline matrices (high quantum yield, absence of spectral diffusion and blinking) but, at the same time, strong inhomogeneous broadening. Moreover, the spectral density of SMs features a fine structure which strongly depends on the history of sample preparation. We wish to emphasize, however, that the dynamical behavior of the vast majority of SM spectra in all samples exhibit crystal-like behavior: they show no spectral jumps, splitting, or blinking. The laser intensity in our measurements was adjusted in the range $\sim 1\text{--}3$ W cm^{-2} , for which light-induced processes were negligible.

The total duration of the measurements on Tr/*o*-DCB was about 8 hours. As in the case of Tr/*n*-Hex, the “pure recording time” was shorter, about 5 h 50 min. Taking into account the SM spectral linewidths of Tr/*o*-DCB at $T = 1.5$ K (30–200 MHz), this corresponds to typical recording times of a SM spectral line of 30–200 ms.

The inhomogeneous absorption band of Tr/*o*-DCB has a quasi-site structure, which is best resolved in the SM spectral density $N_{\text{SM}}(\tilde{\nu})$ (see Fig. 5a). The bulk fluorescence excitation spectrum $F(\tilde{\nu})$ is structureless (gray line in Fig. 5b). We ascribe its poorly resolved structure to the fluorescence emission of non-resonantly excited SMs. Such an unstructured inhomogeneous profile can be modeled according to ref. 74 and ref. 75, where it was calculated as the sum of a set of spectral sub-bands. Each sub-band was composed of the narrow ZPLs of all resonantly excited molecules corresponding to $A_{\text{sum}}(\tilde{\nu})$ and the broad PSBs of non-resonant chromophores.

The average SM linewidth $\bar{\gamma}(\tilde{\nu})$ and the average peak fluorescence signal $\bar{I}_{\text{max}}(\tilde{\nu})$ (Fig. 5c and d; both smoothed over 20 scan segments) are increasing from the red to the blue edge of the band. A similar trend had been observed in FLN measurements for Eu^{3+} ions in an amorphous silicate many years ago.⁶³ Our new technique of recording numerous SM spectra allows us to discover such correlations as well, but on the qualitatively new (all single dye molecules) level.

Fig. 6d,c shows the linewidth histogram of all detected Tr molecules in the *o*-DCB sample. An interesting result is obtained when we plot the spatial arrangement of a subset of SMs in a given linewidth interval and compare it to that of all recorded molecules (Fig. 6b). As an example we selected chromophores with linewidths broader than 120 MHz. The corresponding topograms showing the color-encoded spatial

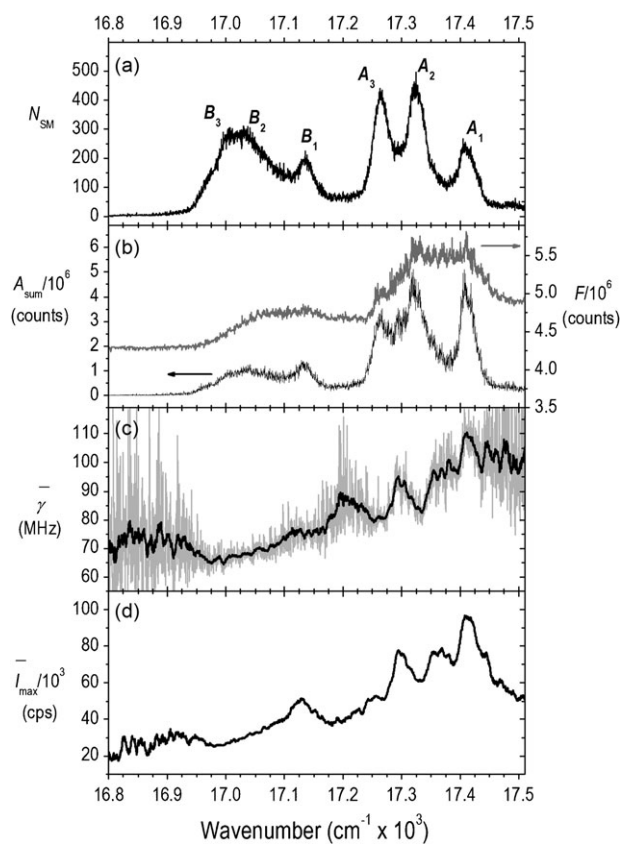


Fig. 5 Arrangement of zero-phonon lines in the inhomogeneous absorption band and corresponding distributions of their spectral parameters for 286 931 single terrylene molecules in *o*-dichlorobenzene. $T = 1.5$ K; scan segment, $\Delta\tilde{\nu} = 10$ GHz. (a) Spectral density of SMs $N_{SM}(\tilde{\nu})$; (b) phononless absorption band $A_{sum}(\tilde{\nu})$ (black line, left scale) and fluorescence excitation spectrum $F(\tilde{\nu})$ (gray line, right scale); (c) average linewidth of the SM spectra $\bar{\gamma}(\tilde{\nu})$ (gray line) and smoothed over 20 segments (black line); (d) average peak count rate of the SM spectra $\bar{I}_{max}(\tilde{\nu})$ smoothed over 20 segments.⁵¹

density are presented in Fig. 6c (all linewidths) and Fig. 6d (linewidths > 120 MHz). The most pronounced difference between the two panels is a small area at the 11 o'clock position where Tr molecules with very broad lines are present at higher concentration, although the overall chromophore density is not unusually high. Perhaps *o*-DCB exhibits some kind of polymorphism which leads to the formation of regions in a particularly disordered or glassy state (see, *e.g.*, ref. 76). Disordered regions in the host matrix manifest themselves mainly by the presence of broad lines of dopant chromophores due, *e.g.*, to local difference of electron-phonon coupling characteristics and/or to fast spectral-diffusion processes (although slow spectral-diffusion events could not be temporally resolved). In topograms color-encoding the spectral line positions (see Fig. 2c and 4 in ref. 51), on the other hand, this area does not show any peculiarities. Thus, the linewidth of SM spectra is an additional experimental parameter which yields valuable information about the matrix.

One more interesting feature of the investigated sample of Tr/*o*-DCB is related to the histogram of the SM peak fluorescence count rate $\bar{I}_{max}(\tilde{\nu})$ at different positions in the

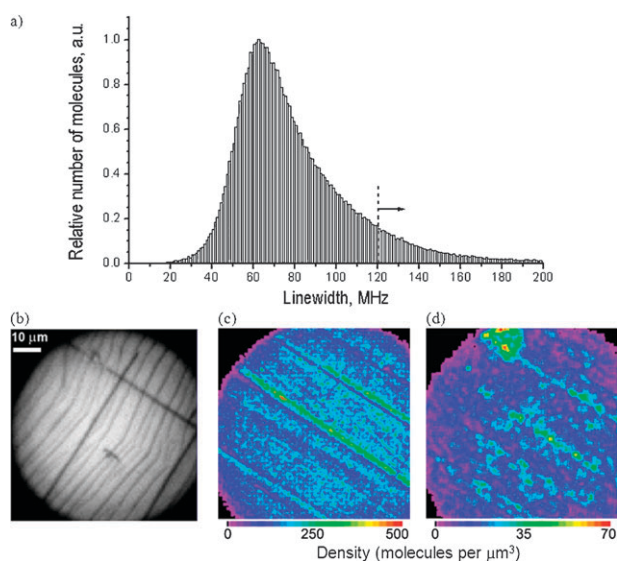


Fig. 6 (a) Distribution of the zero-phonon linewidths of all 286 931 single terrylene molecules in *o*-dichlorobenzene. (b) Photograph of the sample under white-light illumination from the back side. (c) Color-encoded topogram representing the area density of all detected Tr molecules in the sample plane. (d) Same as (c) for those Tr molecules with linewidths broader than 120 MHz (compare part (a)). A pronounced feature in the image is the small area close to the edge of the sample (at the 11 o'clock position), where Tr molecules with broad lines are particularly concentrated.

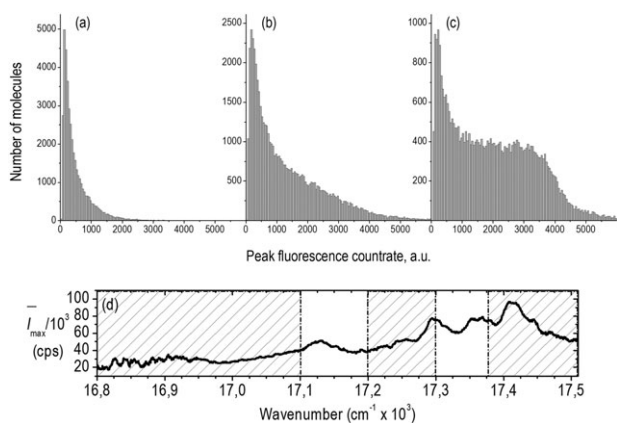


Fig. 7 Distributions of the peak fluorescence intensity I_{max} for single Tr molecules whose ZPLs are located in different spectral regions: (a) 16 800–17 100 cm^{-1} ; (b) 17 200–17 300 cm^{-1} ; (c) 17 375–17 500 cm^{-1} . Note the different scales of the ordinate axis. Part (d) shows the average peak count rate of the SM spectra $\bar{I}_{max}(\tilde{\nu})$ (Fig. 5d) for comparison again.

inhomogeneous band. According to Fig. 5d, the frequency dependence of the average value $\bar{I}_{max}(\tilde{\nu})$ shows strong variations across the band. It reaches local maxima at sites A_1 and B_1 , but also in the regions between A_1 and A_2 and between A_2 and A_3 .

Additional information can be obtained from an analysis of the I_{max} distribution for SMs detected in different spectral ranges. Fig. 7a–c shows these histograms for Tr molecules with ZPLs in the spectral intervals 16 800–17 100 cm^{-1} , 17 200–17 300 cm^{-1} , and 17 375–17 500 cm^{-1} , respectively. Their shape varies with increasing frequency in a pronounced

manner, from a single-peak to a double-peak structure. A possible interpretation may be that there are (at least) two subsets of Tr molecules present in the sample which differ in some properties affecting the fluorescence signal (*e.g.*, the preferential orientation in the matrix). The relative number of chromophores in the subsets then varies with the optical frequency. In addition, the fluorescence count rate is also influenced by the site structure as plotted in Fig. 5d. Between crossed polarizers, however, the sample did not show a pronounced domain structure (data not shown). More detailed information may be obtained by measuring the polarization dependence of the fluorescence signals.⁷⁷

6. Amorphous polyisobutylene doped with tetra-*tert*-butylterrylene

Polyisobutylene ($M_w = 420\,000\text{ g mol}^{-1}$) doped with TBT is one of the most thoroughly studied dye–matrix systems. It has been investigated both with SMS^{32,33,41,53,54,58,59,73} and with the ensemble methods photon echo and hole burning.^{55,56,78}

With our new technique we obtained slow and structureless spectral dependences of the parameters $N_{\text{SM}}(\tilde{\nu})$, $A_{\text{sum}}(\tilde{\nu})$, and $F(\tilde{\nu})$ (time of the measurements, $\sim 7\text{ h}$; pure recording time, $\sim 4\text{ h}$; time per SM spectral line, 50–500 ms). The functions coincide with the fluorescence excitation and absorption spectra of bulk samples as measured in ref. 33 and ref. 78 (apart from a slight shift to lower frequencies; Fig. 8). We found no pronounced spectral variations of the average linewidth $\bar{\gamma}(\tilde{\nu})$ and the average maximum fluorescence count rate $\bar{I}_{\text{max}}(\tilde{\nu})$ either, in striking contrast to Tr/*o*-DCB (*cf.* Fig. 5). Hence, there are no indications for the existence of micro-sites in TBT/PIB. All SM lines exhibit slow spectral dynamics (jumps, splitting). These characteristics are typical for a completely amorphous system, both at the ensemble and the SM level.

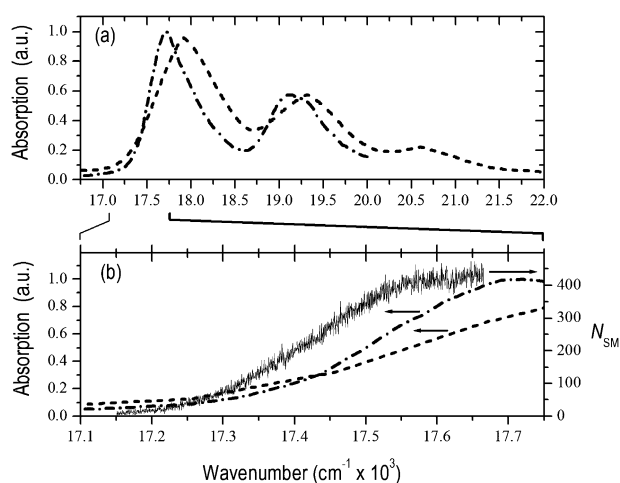


Fig. 8 Inhomogeneous absorption band of amorphous polyisobutylene doped with tetra-*tert*-butylterrylene as measured with different techniques. (a, b) Fluorescence excitation (*dash-dotted lines*) and absorption spectrum (*dashed lines*) measured on bulk samples in ref. 33 and ref. 78, respectively. The solid line in (b) represents the spectral density $N_{\text{SM}}(\tilde{\nu})$ of 328 752 single TBT molecules in the red part of the inhomogeneous band as obtained in the present study. $T = 1.5\text{ K}$.

In this context we would like to discuss a limitation of our technique which is related to the spectral dynamics of SMs. First, this dynamics (spectral jumps, blinking, and/or splitting) leads to errors when SM spectra are fitted with Lorentz (or other simple analytical) functions, hence affecting the recognition and identification procedure of SM spectraspectra (see *e.g.* ref. 59). In the case of TBT/PIB ($420\,000\text{ g mol}^{-1}$), however, this effect is negligible at $T = 1.5\text{ K}$, considering typical recording times of SM spectra of a few ten milliseconds. The second problem is that, in the presence of spectral jumps, the same molecule may be recorded more than once. To avoid this effect it would be useful to measure the temporal evolution of SM spectra (*i.e.*, spectral trails), as was done in our other studies.⁷⁹ If hundreds of thousands of SM spectral trails are to be recorded, on the other hand, the procedure requires unreasonably long measuring times, so it was not performed here. We can also note that spectral-diffusion processes in equilibrium do not affect the dependence $N_{\text{SM}}(\tilde{\nu})$, since equal numbers of SM spectra jump into and out of a scan segment during the recording time of this segment. Hence, the number of molecules which are counted repeatedly is equal to the number of those which are not counted at all.

The comparison of the data measured for Tr/*n*-Hex, Tr/*o*-DCB and TBT/PIB (Fig. 3–8, respectively) impressively demonstrates that the “synthetic” distributions $N_{\text{SM}}(\tilde{\nu})$, $A_{\text{sum}}(\tilde{\nu})$, $\bar{\gamma}(\tilde{\nu})$, and $\bar{I}_{\text{max}}(\tilde{\nu})$, which are based on ZPL recognition and are not affected by the broad PSBs, reveal a vast amount of additional information about the local structure of disordered solids. These details are usually hidden in the bulk fluorescence excitation spectrum $F(\tilde{\nu})$ to a large degree.

7. Conclusions

We have presented the results of measurements and detailed analyses of the individual fluorescence excitation spectra and lateral coordinates for huge ensembles (hundreds of thousands and more) of single impurity molecules in low-temperature solids. Our technique involves massively parallel recording of the zero-phonon lines of single-molecule spectra with a CCD camera and the storage of all their spectral parameters for further analysis. We applied it to the comparative study of two polycrystalline solids, *n*-hexadecane and *o*-dichlorobenzene both doped with terrylene, which exhibit very different photo-physical properties, and the amorphous polymer polyisobutylene doped with TBT.

For the three systems we have found how the electronic zero-phonon lines of individual chromophores are distributed across the inhomogeneous band. It was demonstrated that this approach is fundamentally more informative than conventional high-resolution fluorescence excitation spectroscopy. The spectral densities of ZPLs have, at least in crystalline matrices, distinctly more pronounced structures, since they are not blurred by fluorescence signals of non-resonant impurities excited *via* their phonon sidebands. Also the dependence of other spectral parameters of SMs (*e.g.*, linewidth and maximum fluorescence count rate) on the frequency position in the absorption band was analyzed, and

distinct correlations were found. In the system Tr/o-DCB we discovered correlations between the linewidths and the spatial positions of the dye molecules. A small area of the sample showed an accumulation of particularly broad lines.

To glean the full information about a dye–matrix system, it is necessary to record and evaluate a substantial fraction of all the SM spectra in a given volume. This technique allows us, in principle, to measure the complete optical spectrum of a bulk sample by recording the spectra of (nearly) all individual molecules contributing to it. In a sense it leads us close to the ultimate goal of the optical spectroscopy of impurity centers, obtaining local spectroscopic data free from ensemble averaging (as obtained *via* SMS) and linking it to the macroscopic properties of a solid.

Acknowledgements

Financial support from the Deutsche Forschungsgemeinschaft (Collaborative Research Centre [SFB] 481 and grants Ko 1359/14 and 436 RUS 17/102/06) is gratefully acknowledged. The Russian team acknowledges also financial support from the Russian Foundation of Basic Research (08-02-00147, 10-02-90047, 11-02-00816), Russian State Contracts (02.740.11.0431; 02.740.11.0870). A.V. Naumov is grateful for a Grant of the President of Russia (MD-3191.2009.2).

References and notes

- M. Orrit, J. Bernard and R. I. Personov, *J. Phys. Chem.*, 1993, **97**, 10256–10268.
- E. V. Shpol'skii, A. A. Il'ina and L. A. Klimova, *Dokl. Akad. Nauk UzSSR*, 1952, **57**, 935.
- E. V. Shpol'skii, *Soviet Physics Uspekhi*, 1963, **80**, 255.
- K. K. Rebane, *Impurity Spectra of Solids; Elementary Theory of Vibrational Structure*, Plenum Press, New York, 1970.
- R. I. Personov, E. L. Al'shits and L. A. Bykovskaja, *JETP Lett.*, 1972, **15**, 431.
- V. M. Agranovich and R. M. Hochstrasser, *Spectroscopy and Excitation Dynamics of Condensed Molecular Systems*, North-Holland Pub. Co., Sole distributors for the USA and Canada, Elsevier Science Pub. Co., Amsterdam, New York, 1983.
- B. M. Kharlamov, R. I. Personov and L. A. Bykovskaya, *Opt. Commun.*, 1974, **12**, 191.
- A. A. Gorokhovskii, R. K. Kaarli and L. A. Rebane, *JETP Lett.*, 1974, **20**, 474.
- W. E. Moerner and L. Kador, *Phys. Rev. Lett.*, 1989, **62**, 2535–2538.
- M. Orrit and J. Bernard, *Phys. Rev. Lett.*, 1990, **65**, 2716–2719.
- S. Völker, *Annu. Rev. Phys. Chem.*, 1989, **40**, 499–530.
- B. Henderson, *Contemp. Phys.*, 2002, **43**, 273–300.
- D. J. Norris, A. L. Efros, M. Rosen and M. G. Bawendi, *Phys. Rev. B: Condens. Matter*, 1996, **53**, 16347–16354.
- S. P. Feofilov, A. A. Kaplyanskii, R. I. Zakharchenya, Y. Sun, K. W. Jang and R. S. Meltzer, *Phys. Rev. B: Condens. Matter*, 1996, **54**, R3690–R3693.
- J. Zollfrank, J. Friedrich, J. M. Vanderkooi and J. Fidy, *J. Chem. Phys.*, 1991, **95**, 3134–3136.
- J. Gafert, H. Pschierer and J. Friedrich, *Phys. Rev. Lett.*, 1995, **74**, 3704–3707.
- Y. Shibata, A. Kurita and T. Kushida, *J. Chem. Phys.*, 1996, **104**, 4396–4405.
- Y. Berlin, A. Burin, J. Friedrich and J. Köhler, *Phys. Life Rev.*, 2006, **3**, 262–292.
- H. M. Wu, M. Rätsep, I. J. Lee, R. J. Cogdell and G. J. Small, *J. Phys. Chem. B*, 1997, **101**, 7654–7663.
- F. Ariese, A. N. Bader and C. Gooijer, *TrAC, Trends Anal. Chem.*, 2008, **27**, 127–138.
- P. Esquinazi, *Tunneling Systems in Amorphous and Crystalline Solids*, Springer, Berlin, New York, 1998.
- U. Buchenau, M. Prager, N. Nucker, A. J. Dianoux, N. Ahmad and W. A. Phillips, *Phys. Rev. B: Condens. Matter*, 1986, **34**, 5665–5673.
- U. P. Wild, F. Güttler, M. Pirodda and A. Renn, *Chem. Phys. Lett.*, 1992, **193**, 451–455.
- T. Plakhotnik, E. A. Donley and U. P. Wild, *Annu. Rev. Phys. Chem.*, 1997, **48**, 181–212.
- Y. Berlin, A. Burin, J. Friedrich and J. Köhler, *Phys. Life Rev.*, 2007, **4**, 64–89.
- W. E. Moerner and M. Orrit, *Science*, 1999, **283**, 1670–1676.
- X. S. Xie and J. K. Trautman, *Annu. Rev. Phys. Chem.*, 1998, **49**, 441–480.
- J. Köhler, *Phys. Rep.*, 1999, **310**, 262–339.
- E. Barkai, Y. J. Jung and R. Silbey, *Annu. Rev. Phys. Chem.*, 2004, **55**, 457–507.
- F. Kulzer and M. Orrit, *Annu. Rev. Phys. Chem.*, 2004, **55**, 585–611.
- A. V. Naumov and Yu. G. Vainer, *Phys.-Usp.*, 2009, **52**, 298–304.
- B. Kozankiewicz, J. Bernard and M. Orrit, *J. Chem. Phys.*, 1994, **101**, 9377–9383.
- R. Kettner, J. Tittel, T. Basché and C. Bräuchle, *J. Phys. Chem.*, 1994, **98**, 6671–6674.
- J. Tittel, R. Kettner, T. Basché, C. Bräuchle, H. Quante and K. Müllen, *J. Lumin.*, 1995, **64**, 1–11.
- E. Geva and J. L. Skinner, *J. Phys. Chem. B*, 1997, **101**, 8920–8932.
- E. A. Donley, V. Burzomato, U. P. Wild and T. Plakhotnik, *J. Lumin.*, 1999, **83–84**, 255–259.
- E. A. Donley, H. Bach, U. P. Wild and T. Plakhotnik, *J. Phys. Chem. A*, 1999, **103**, 2282–2289.
- E. Barkai, R. Silbey and G. Zumofen, *Phys. Rev. Lett.*, 2000, **84**, 5339–5342.
- Yu. G. Vainer, A. V. Naumov, M. Bauer, L. Kador and E. Barkai, *Opt. Spectrosc.*, 2005, **98**, 740–746.
- Yu. G. Vainer and A. V. Naumov, *Opt. Spectrosc.*, 2005, **98**, 747–752.
- Yu. G. Vainer, A. V. Naumov, M. Bauer and L. Kador, *Phys. Rev. Lett.*, 2006, **97**, 185501.
- J. Sepiol, J. Jasny, J. Keller and U. P. Wild, *Chem. Phys. Lett.*, 1997, **273**, 444–448.
- J. Jasny, J. Sepiol, T. Irngartinger, M. Traber, A. Renn and U. P. Wild, *Rev. Sci. Instrum.*, 1996, **67**, 1425–1430.
- M. J. Rust, M. Bates and X. W. Zhuang, *Nat. Methods*, 2006, **3**, 793–795.
- E. Betzig, G. H. Patterson, R. Sougrat, O. W. Lindwasser, S. Olenych, J. S. Bonifacio, M. W. Davidson, J. Lippincott-Schwartz and H. F. Hess, *Science*, 2006, **313**, 1642–1645.
- M. Heilemann, S. van de Linde, M. Schüttelpe, R. Kasper, B. Seefeldt, A. Mukherjee, P. Tinnefeld and M. Sauer, *Angew. Chem., Int. Ed.*, 2008, **47**, 6172–6176.
- M. Bates, B. Huang, G. T. Dempsey and X. W. Zhuang, *Science*, 2007, **317**, 1749–1753.
- A. M. van Oijen, J. Köhler, J. Schmidt, M. Müller and G. J. Brakenhoff, *Chem. Phys. Lett.*, 1998, **292**, 183–187.
- A. M. van Oijen, J. Köhler, J. Schmidt, M. Müller and G. J. Brakenhoff, *J. Opt. Soc. Am. A*, 1999, **16**, 909–915.
- T. Yu. Lатыchevskaja, A. Renn and U. P. Wild, *J. Lumin.*, 2006, **118**, 111–122.
- A. V. Naumov, A. A. Gorshelev, Yu. G. Vainer, L. Kador and J. Köhler, *Angew. Chem., Int. Ed.*, 2009, **48**, 9747–9750.
- A. Bohnen, K. H. Koch, W. Lüttke and K. Müllen, *Angew. Chem., Int. Ed. Engl.*, 1990, **29**, 525–527.
- A. V. Naumov, Yu. G. Vainer, M. Bauer, S. Zilker and L. Kador, *Phys. Rev. B: Condens. Matter Mater. Phys.*, 2001, **63**, 212302.
- A. V. Naumov, Yu. G. Vainer, M. Bauer and L. Kador, *Phys. Status Solidi B*, 2004, **241**, 3487–3492.
- Yu. G. Vainer, M. A. Kol'chenko, A. V. Naumov, R. I. Personov and S. J. Zilker, *J. Lumin.*, 2000, **86**, 265–272.
- Yu. G. Vainer, A. V. Naumov, M. A. Kol'chenko and R. I. Personov, *Phys. Status Solidi B*, 2004, **241**, 3480–3486.
- The original algorithms and computer software for quick automatic spectral images recognition, data processing and spectral-spatial correlations finding (© 2007, A.V. Naumov, Troitsk, Moscow region, Russia).
- A. V. Naumov, Yu. G. Vainer and L. Kador, *Phys. Rev. Lett.*, 2007, **98**, 145501.

- 59 Yu. G. Vainer, A. V. Naumov, M. Bauer and L. Kador, *J. Lumin.*, 2007, **127**, 213–217.
- 60 Yu. G. Vainer, A. V. Naumov and L. Kador, *Phys. Rev. B: Condens. Matter Mater. Phys.*, 2008, **77**, 224202.
- 61 E. Lang, J. Baier and J. Köhler, *J. Microsc.*, 2006, **222**, 118–123.
- 62 L. Kador, P. Geissinger and D. Haarer, *J. Lumin.*, 1995, **64**, 101–107.
- 63 P. Avouris, A. Campion and M. A. El Sayed, *J. Chem. Phys.*, 1977, **67**, 3397.
- 64 N. Hartmannsgruber and M. Maier, *J. Chem. Phys.*, 1992, **96**, 7279–7286.
- 65 A. A. L. Nicolet, C. Hofmann, M. A. Kol'chenko, B. Kozankiewicz and M. Orrit, *ChemPhysChem*, 2007, **8**, 1215–1220.
- 66 M. Vacha, Y. Liu, H. Nakatsuka and T. Tani, *J. Chem. Phys.*, 1997, **106**, 8324–8331.
- 67 H. Bach, E. A. Donley, M. Traber, A. Renn and U. P. Wild, *Opt. Mater. (Amsterdam)*, 1998, **9**, 376–380.
- 68 Y. Durand, A. Bloëß, A. M. van Oijen, J. Köhler, E. J. J. Groenen and J. Schmidt, *Chem. Phys. Lett.*, 2000, **317**, 232–237.
- 69 Y. Durand, A. Bloëß, J. Köhler, E. J. J. Groenen and J. Schmidt, *J. Chem. Phys.*, 2001, **114**, 6843–6850.
- 70 A. Bloëß, Y. Durand, M. Matsushita, R. Verberk, E. J. J. Groenen and J. Schmidt, *J. Phys. Chem. A*, 2001, **105**, 3016–3021.
- 71 W. E. Moerner, T. Plakhotnik, T. Irrgartinger, M. Croci, V. Palm and U. P. Wild, *J. Phys. Chem.*, 1994, **98**, 7382–7389.
- 72 A. Sigl, M. Orrit, T. Reinot, R. Jankowiak and J. Friedrich, *J. Chem. Phys.*, 2007, **127**, 084510–084517.
- 73 A. A. Gorshelev, A. V. Naumov, I. Y. Eremchev, Yu. G. Vainer, L. Kador and J. Köhler, *ChemPhysChem*, 2010, **11**, 182–187.
- 74 N. L. Naumova, I. A. Vasil'eva, I. S. Osad'ko and A. V. Naumov, *Opt. Spectrosc.*, 2005, **98**, 535–542.
- 75 N. L. Naumova, I. A. Vasil'eva, A. V. Naumov and I. S. Osad'ko, *J. Lumin.*, 2005, **111**, 37–45.
- 76 M. A. Ramos, I. M. Shmyt'ko, E. A. Arnautova, R. J. Jimenez-Rioboo, V. Rodriguez-Mora, S. Vieira and M. J. Capitan, *J. Non-Cryst. Solids*, 2006, **352**, 4769–4775.
- 77 C. Hofmann, M. Ketelaars, M. Matsushita, H. Michel, T. J. Aartsma and J. Köhler, *Phys. Rev. Lett.*, 2003, **90**, 013004.
- 78 S. J. Zilker, D. Haarer and Yu. G. Vainer, *Chem. Phys. Lett.*, 1997, **273**, 232–238.
- 79 I. Y. Eremchev, Yu. G. Vainer, A. V. Naumov and L. Kador, *Phys. Chem. Chem. Phys.*, 2010, DOI: 10.1039/c0cp01690j.